Research article

Ionic self-complementarity induces amyloid-like fibril formation in an isolated domain of a plant copper metallochaperone protein

Helena Mira[†1], Marçal Vilar[†1], Vicent Esteve[1], Marc Martinell[2], Marcelo J Kogan[2], Ernest Giralt[2,3], David Salom[4], Ismael Mingarro[1], Lola Peñarrubia[1] and Enrique Pérez-Payá[*1,5]

Address: [1]Departament de Bioquímica i Biologia Molecular, Universitat de València. E-46100 Burjassot, València, Spain, [2]Institut de Recerca Biomèdica de Barcelona (IRBB-PCB), Universitat de Barcelona, E-08028 Barcelona, Spain, [3]Departament de Química Orgànica, Universitat de Barcelona. E-08028 Barcelona, Spain, [4]Department of Biochemistry and Biophysics. University of Pennsylvania. Philadelphia, PA 19104-6059, USA. Current address: Novasite Pharmaceuticals, 11095 Flintkote Ave., San Diego, CA 92121, USA and [5]Fundación Valenciana de Investigaciones Biomédicas, CSIC. E-46010 València, Spain

Email: Helena Mira - helena.mira@uv.es; Marçal Vilar - marcial.vilar@uv.es; Vicent Esteve - vicent.esteve@uv.es; Marc Martinell - mmartinell@pcb.ub.es; Marcelo J Kogan - mkogan@pcb.ub.es; Ernest Giralt - egiralt@pcb.ub.es; David Salom - dsalom@novasite.com; Ismael Mingarro - ismael.mingarro@uv.es; Lola Peñarrubia - lola.penarrubia@uv.es; Enrique Pérez-Payá* - eperez@ochoa.fib.es

* Corresponding author †Equal contributors

Abstract

Background: *Arabidopsis thaliana* copper metallochaperone CCH is a functional homologue of yeast antioxidant ATX1, involved in cytosolic copper transport. In higher plants, CCH has to be transported to specialised cells through plasmodesmata, being the only metallochaperone reported to date that leaves the cell where it is synthesised. CCH has two different domains, the N-terminal domain conserved among other copper-metallochaperones and a C-terminal domain absent in all the identified non-plant metallochaperones. The aim of the present study was the biochemical and biophysical characterisation of the C-terminal domain of the copper metallochaperone CCH.

Results: The conformational behaviour of the isolated C-domain in solution is complex and implies the adoption of mixed conformations in different environments. The ionic self-complementary peptide KTEAETKTEAKVDAKADVE, derived from the C-domain of CCH, adopts and extended conformation in solution with a high content in β-sheet structure that induces a pH-dependent fibril formation. Freeze drying electron microscopy studies revealed the existence of well ordered amyloid-like fibrils in preparations from both the C-domain and its derivative peptide.

Conclusion: A number of proteins related with copper homeostasis have a high tendency to form fibrils. The determinants for fibril formation, as well as the possible physiological role are not fully understood. Here we show that the plant exclusive C-domain of the copper metallochaperone CCH has conformational plasticity and forms fibrils at defined experimental conditions. The putative influence of these properties with plant copper delivery will be addressed in the future.

Background

Apparently natural β-sheet proteins seem to avoid aggregation by disfavouring solvent exposed sequences that could drive intermolecular aggregation [1]. In fact, most

of the natural proteins forming fibrillar aggregates are related to a range of human metabolic disorders [2]. Among the aggregation processes, the amyloidosis is a group of protein misfolding disorders characterized by the formation of fibrils [2]. Although most of these processes have been described in humans, other organisms also present examples of proteins forming amyloid fibrils, such as monellin from higher plants [3,4]. However, the physiological relevance of the aggregation processes remains obscure. A number of these amyloid forming proteins are involved in copper homeostasis, and oxidative damage induced by copper may play a role in the pathogenesis of neurodegenerative conditions. β-amyloid (Aβ), implicated in the pathogenesis of Alzheimer's disease, forms an oligomeric complex that binds Cu^{2+} with very high affinity forming an allosterically cooperative Cu^{2+}-coordination site that resembles superoxide dismutase 1 (SOD) [5]. Aggregation of SOD has also been related to familial amyotrophic lateral sclerosis (ALS) [6] and copper-bound prion protein (PrP) [7,8] shows superoxide dismutase activity [9].

The present study describes the amyloidosis properties of the C-terminal domain of the *Arabidopsis thaliana* copper metallochaperone CCH, which is a functional homologue of the cytosolic metallochaperone antioxidant 1 (Atx1) [10] from the yeast *Saccharomyces cerevisiae*. Atx1 delivers copper to transporters at a post-Golgi compartment to load the ion at cuproproteins in the secretory pathway [11,12]. CCH has been found in plant vascular tissues where its concentration increases greatly during senescence [13] and it is mainly located in cells that lack their nuclei and therefore they could be unable of DNA transcription or translation. Consequently, CCH should be transported from neighbour cells through plasmodesmata, being the only metallochaperone reported to date that could leave the cell where it is synthesised [13]. CCH (121 residues) has two different domains with independent folding pathways [14]. The conserved N-terminal domain (amino acids 1–68, referred herein as the N-domain) contains the copper-binding motif MXCXXC that retains both, the overall "open-faced β-sandwich" fold and the copper chaperone and antioxidant properties described for the yeast Atx1 [14]. The C-terminal domain (amino acids 69–121, the C-domain), is absent in all the identified non-plant metallochaperones [10], displayed altered SDS/PAGE mobility and it adopts an extended (beta) conformation in solution and in the presence of anionic detergents. Thus, we have postulated that the CCH extra C-domain participates in this plant-exclusive copper transport mechanism. The C-domain has structural features that could favour the adoption of an extended structure in β-sheet conformation. It is characterized by two repeats (Fig. 1) that have a binary structural periodicity of polar/non polar amino acids along the sequence with potential to adopt β-sheet structures that self-assembled into large oligomers [15,16]. In this report we have addressed the structural characterization of the C-domain. The conformational behaviour of the molecule in solution is complex and implies the adoption of mixed conformations in different environments. In an increasing number of proteins, the understanding of the folding mechanism could be addressed by means of the analysis of short polypeptide segments [17-20]. Thus a fruitful approach to investigate the autonomous folding and function of protein subdomains is the design and structural characterization of simplified peptide models that could reproduce the molecular characteristics of the whole protein domain. In the present study, we have selected the peptide, K^{90}TEAETKTEAKVDAKADVE^{108} derived from the C-domain of CCH, since it contains a segment of alternating hydrophobic and hydrophilic residues and a striking overall charge distribution (Fig. 1). The peptide adopts an extended conformation in solution with a high content in β-sheet structure that induces a pH-dependent fibril formation. Freeze drying electron microscopy studies revealed the existence of well ordered amyloid-like fibrils in preparations from both the C-domain and its derivative peptide. The results showed that polypeptides containing complementary charges promote fibril formation, not only in *de novo* designed peptides [21,22] but also in polypeptides derived from natural existing proteins. Furthermore, the relevance of the self-assembly properties of the C-domain of CCH is discussed in the context of plasmodesmata trafficking through microtubules and other putative functions related to the role of its ortologues.

Results

The recombinant C-domain of CCH, expressed and purified from *Escherichia coli*, has been shown to have an altered electrophoretic mobility in SDS-PAGE and its preliminary structural characterization suggested that it could adopt an extended β-sheet structure in solution at neutral pH [14]. The amino acid sequence of the C-domain is characterized by the presence of two segments of binary structural periodicity of polar/non polar amino acids (Fig. 1A). Provided that 22 out of 30 polar residues are Asp, Glu and Lys, the conformational behaviour of the C-domain could be influenced by ionic self-complementarity that has been early described as a property that confers multifaceted behaviour in model peptides and that could induce fibril formation [22]. In fact the polypeptide that defines the C-domain showed a complex behaviour in solution with the coexistence of monomeric and large oligomeric conformations. The presence in salt-free aqueous solution of large fibril-like aggregates was demonstrated by freeze fixation, freeze drying transmission electron microscopy imaging (TEM) (Fig. 2). A recombinant C-domain polypeptide solution was prepared and divided

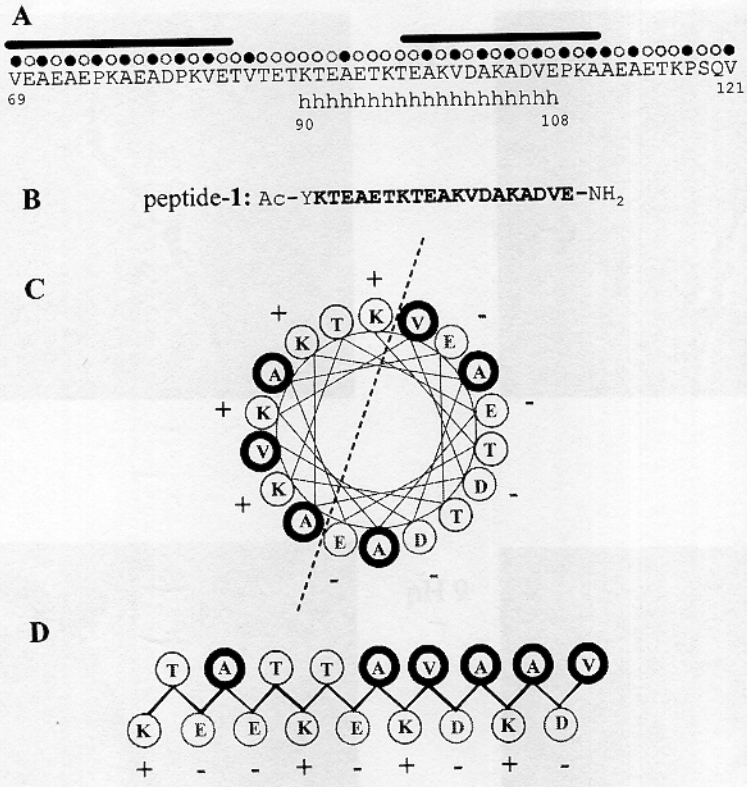

Figure 1

Representation of the C-domain of the CCH protein and related synthetic peptides. (A). Amino acid sequence (one letter code) of the C-domain (residues 69–121) of CCH. The sequence shows relative alternating periodicity of nonpolar (●) and polar (○) amino acids. The stretch of 'h' indicates the putative α-helix predicted by secondary-structure algorithms. The bars denote the location of the two 16-residue repeats of binary structural periodicity of polar/non polar amino acids. **(B).** Such a motif was used to design the synthetic peptide-**1**. The amino acid sequence of peptide-**1** is arranged into an α-helix **(C)** and into a β-sheet conformation **(D).** Positively and negatively charged amino acids are in blue and red, respectively and hydrophobic amino acids are bold cycled.

in four fractions adjusted with HCl or NaOH at different pH values. At pH 7 and 9 the fibrils are long and unbranched while at pH 3 and 5 they showed irregular shapes. As previously mentioned, the recombinant CCH C-domain has been shown to present an altered mobility in SDS-PAGE gels [14]. Electrophoretic mobilities on SDS-PAGE uncorrelated to protein molecular masses, have been described as a result of intrinsic net charge, SDS-induced protein conformation and/or SDS-resistant oligomerization [23-26]. We first examined the aggregation state of recombinant CCH C-domain by sedimentation equilibrium at three different protein concentrations in 50 mM Tris-HCl buffer pH 8.0 containing 0.2 M NaCl that precludes the oligomerization of the polypeptide induced by ionic self-complementarity (Fig. 3A). Three data sets were fit simultaneously to a single species model, with molecular weight as a global fitting parameter. The experimental molecular weight obtained was 4910 ± 140 Da, which fits well to the expected value of 4936.5 Da derived from the amino acid sequence of the C-domain. However, these results differ from the molecular weight obtained in SDS-PAGE for the recombinant C-domain [14]. Since SDS has been described as a membrane mimetic agent prone to induce peptide conformational changes [27] that in turn can modify protein-protein interactions, it is possible that SDS could orchestrate conformational changes leading to oligomerization. Therefore, we performed analytical ultracentrifugation in the

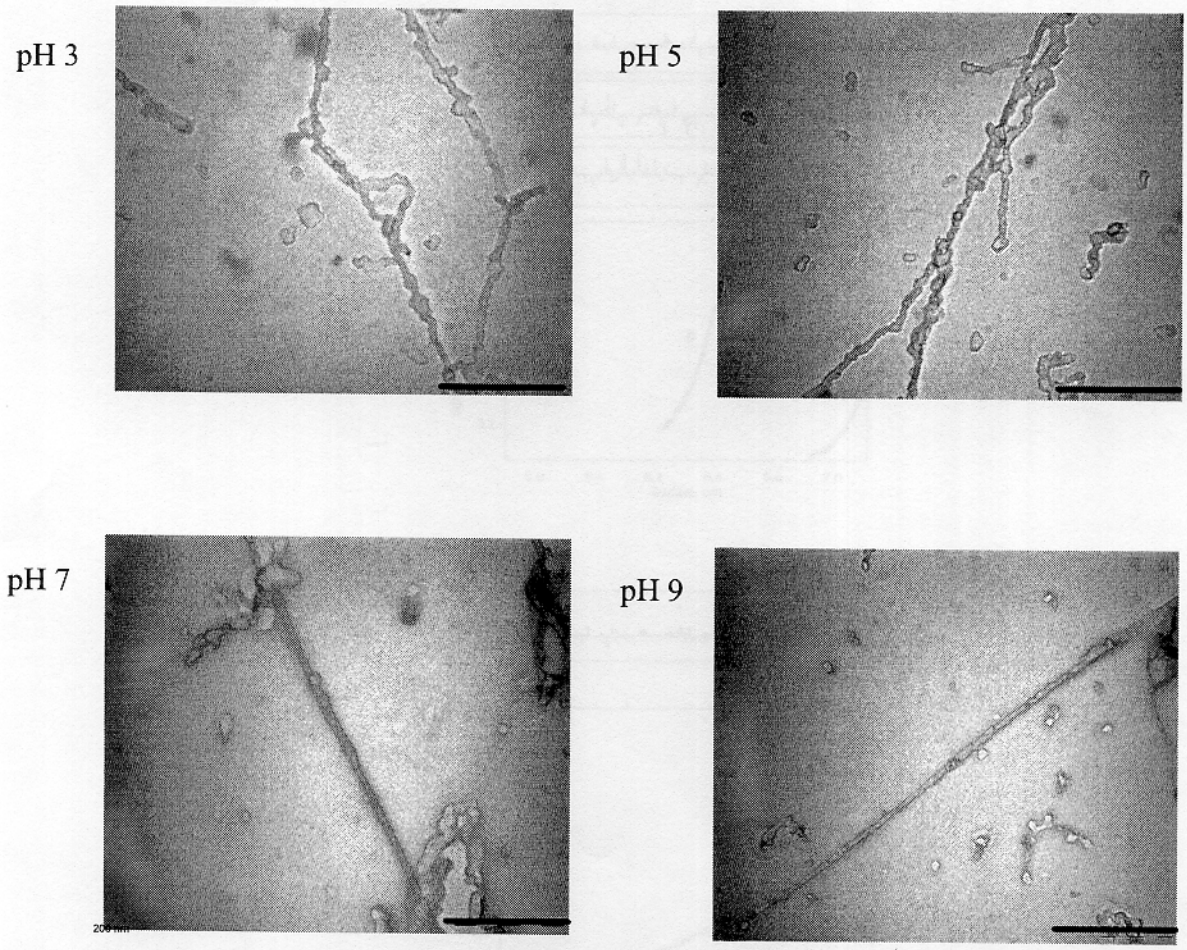

Figure 2
TEM images. TEM images of the replicas obtained after freeze-fixation and freeze-drying of an aqueous solution of recombinant C-domain at different pHs. (Bar = 0.2 μm).

presence of SDS at submicellar concentrations (1 mM), like in the SDS-PAGE experiment. The sedimentation profile of the recombinant C-domain in these conditions (black squares in Fig 3B) did not fit well to a model representing a single species model (not shown). Then we fit the data to a two state equilibrium model (i.e., monomer ↔ *n*-mer) where the aggregation number (*n*) and the equilibrium dissociation constant are the global fitting parameters, and the monomer molecular weight (4936.5 Da) is held constant (solid line in Fig 3B). The result obtained was $n = 7.3 \pm 0.2$, and the equilibrium dissociation constant value suggested the presence of significant amounts of both, monomers and oligomers in the sample. This model, however, must be considered only as an approximation to a more realistic model in which the monomers and oligomers would associate with SDS molecules. No further attempt was made to fit the data to a more complex equilibrium model due to the uncertainty in the stoichiometry of the protein-SDS interaction, and the fact that the C-domain and SDS have different partial specific volumes (0.7404 mL/mg calculated for the C-domain, and 0.859 mL/mg for SDS below critical micelle concentration – [28]). From these results and those obtained in TEM, SDS-PAGE and CD, it could be concluded that the C-domain of CCH protein has tendency to form oligomers in different experimental conditions.

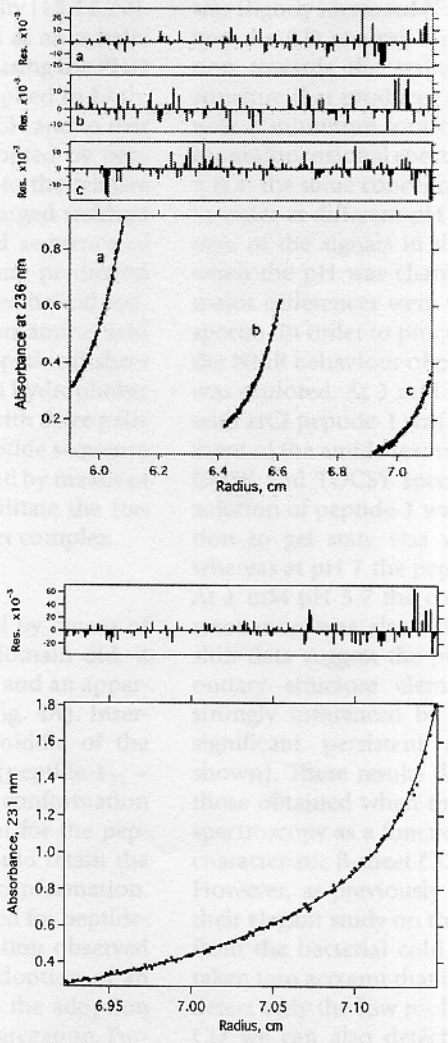

Figure 3

Sedimentation equilibrium analysis of the C-domain. (A). Sedimentation equilibrium of recombinant C-domain at 50000 rpm. Equilibrium A_{280}-radius profiles for three different cell compartments, each one containing the protein at different concentrations. The lines are the best (global) fit to a single species model. The residuals of the fit are shown in the three upper panels.**(B).** Sedimentation equilibrium analysis of the C-domain in the presence of 1 mM SDS. The sample was run at 45000 rpm. The line represents the best fit to a two state equilibrium model. The residuals of the fit are shown in the upper panel.

Selection of a 19-mer peptide model derived from the C-domain of CCH

Since the C-domain showed a complex conformational behaviour in solution, we looked for a simplified peptide model that could facilitate the study of the apparent secondary structure plasticity of the CCH C-domain. We have focused our attention into the sequence KTEAETKTEAKVDAKADVE (amino acids 90 to 108 – Fig. 1A). Then, peptide-**1** is an N-t acetylated, C-t amidated synthetic peptide with such amino acid sequence where a tyrosine residue was placed at the N-terminal end to facilitate quantification by UV spectroscopy (Fig. 1B). Peptide-**1** contains a segment of alternating hydrophobic and hydrophilic residues and a striking overall charge distribu-

tion. These two properties have been early described as determinants for secondary structure plasticity [15,16,22]. In fact, this sequence was predicted to fold as an α-helix by secondary structure prediction methods using the PHD software (EMBL, Heidelberg, Germany) applied to both, to the amino acid sequence of the whole CCH and to that of the C-domain. The putative α-helix adopted by peptide-**1** would show charge segregation due to the relative orientation of positively and negatively charged residues (Fig. 1C). However, when the amino acid sequence of peptide-**1** is analyzed for secondary structure prediction using the program AGADIR [29] the predicted helical content is extremely low. Furthermore, such an amino acid sequence could be arranged into an amphipathic β-sheet conformation (Fig. 1D) that would expose a hydrophobic face and a highly charged hydrophilic face with three pairs Glu-Lys and one pair Asp-Lys. Then, the peptide sequence could be intra- or inter-molecularly stabilized by means of ionic self-complementarity that would facilitate the formation of a macromolecular β-pleated-sheet complex.

Conformational analysis of peptide-1

Peptide-**1** (MW_{teo} = 2267 Da) was analyzed by means of Tris-tricine electrophoresis and, as the C-domain did, it showed an altered electrophoretic mobility and an apparent molecular weight close to 26.6 kDa (Fig. 4A). Insertion of two additional alanines in the middle of the peptide-**1** sequence generates a peptide (peptide-$\mathbf{1}_{22}$ – Table 1) that when plotted in an α-helical conformation would lost the observed charge segregation for the peptide-**1** (Fig. 1C). However, peptide-$\mathbf{1}_{22}$, would retain the capability to adopt an amphipathic β-sheet conformation. The altered electrophoretic mobility obtained for peptide-$\mathbf{1}_{22}$ (Fig. 4A) suggests that the oligomerization observed for these peptides is more related to the adoption of an amphipathic β-sheet conformation than to the adoption of an α-helical conformation with charge segregation. Furthermore, shortened synthetic peptide analogues from peptide-1 with amino acid deletions of two (peptide-$\mathbf{1}_{18}$), six (peptide-$\mathbf{1}_{14}$) and ten (peptide-$\mathbf{1}_{10}$) from the N-terminal (Table 1) were also analysed in order to define the minimum peptide length able to drive oligomerization. Peptide-$\mathbf{1}_{18}$ and peptide-$\mathbf{1}_{14}$, but not peptide-$\mathbf{1}_{10}$, showed altered electrophoretic mobility (data not shown).

The conformational behaviour of peptide-1 in solution at different pHs was analyzed by CD and NMR spectroscopies. At neutral pH and 10 °C (Fig. 4B), the CD spectrum of peptide-**1** is similar to that obtained for the whole C-domain and it is characterized by a strong negative ellipticity band with a minimum at 198 nm characteristic of an extended β-sheet secondary structure. As the temperature increased (from 10–70 °C – insert in Fig. 4B), the spectra showed less intense bands suggesting a decrease in secondary structure. At basic pH values, the negative band at 198 nm of the far-UV CD spectrum obtained at neutral pH was slightly increased (Fig. 4B). However, at acidic pH values, the CD analysis suggested a conformational transition towards the stabilization of a β-sheet secondary structure that produces a canonical β-sheet CD spectrum with a minimum located at 215 nm (Fig. 4B). ^{1}H NMR monodimensional spectra of a 50 μM solution of peptide-1 (i.e. the same concentration used in CD) were acquired in water at different pH values and an increase of dispersion of the signals in the aliphatic region was observed when the pH was changed from 2.7 to 7 (Fig. 4C). No major differences were observed in other regions of the spectra. In order to proceed to chemical shift assignments the NMR behaviour of peptide-**1** at higher concentrations was explored. At 3 mM in water with pH adjusted to 2.5 with HCl peptide-**1** was soluble and the complete assignment of the amide resonances was achieved by analysis of COSY and TOCSY spectra. When the pH of the 3 mM solution of peptide-**1** was raised to 4.5 a reversible transition to gel state was visible on the NMR glass tube, whereas at pH 7 the peptide aggregation was irreversible. At 1 mM pH 5.7 the complete assignment of the amide resonances was also achieved. Secondary α H chemical shift data suggest the putative presence of transient secondary structure elements although the spectra are strongly influenced by peptide conformations without significant persistent secondary structure (data not shown). These results do not correlate, apparently, with those obtained when the peptide-**1** was analysed by CD spectroscopy as a function of pH where different types of characteristic β-sheet CD spectra were obtained (Fig. 4B). However, as previously described by Gross et al. [30] in their elegant study on the aggregation of peptides derived from the bacterial cold shock protein CspB, it must be taken into account that in conventional solution NMR we detect only the low molecular weight species, whereas in CD we can also detect high molecular weight soluble aggregates with a β-sheet structure.

TFE titration of a peptide-1 solution at pH 4.2 induced the stabilization of the β-sheet conformation (Fig. 5A). The CD spectra corresponding to the peptide-**1** either in the absence or in the presence of up to 20% TFE (v/v) showed an isodichroic point at 203 nm that suggested a single conformational transition. However, at TFE concentrations of 40 and 60% (v/v), the spectral characteristics denoted the presence of a mixture of α-helical and β-sheet conformations and the isodichroic point shifted to 201 nm. TFE titration of a solution of peptide-**1** in extended (beta) conformation at pH 6.8 induced the transition towards a canonical β-sheet conformation (Fig. 5B). Thus, at low TFE concentrations (below 20%, v/v) the CD spectra showed a negative ellipticity band at 198 nm, while when the TFE concentration was increased, the CD spectra displayed a single minimum at 215 nm character-

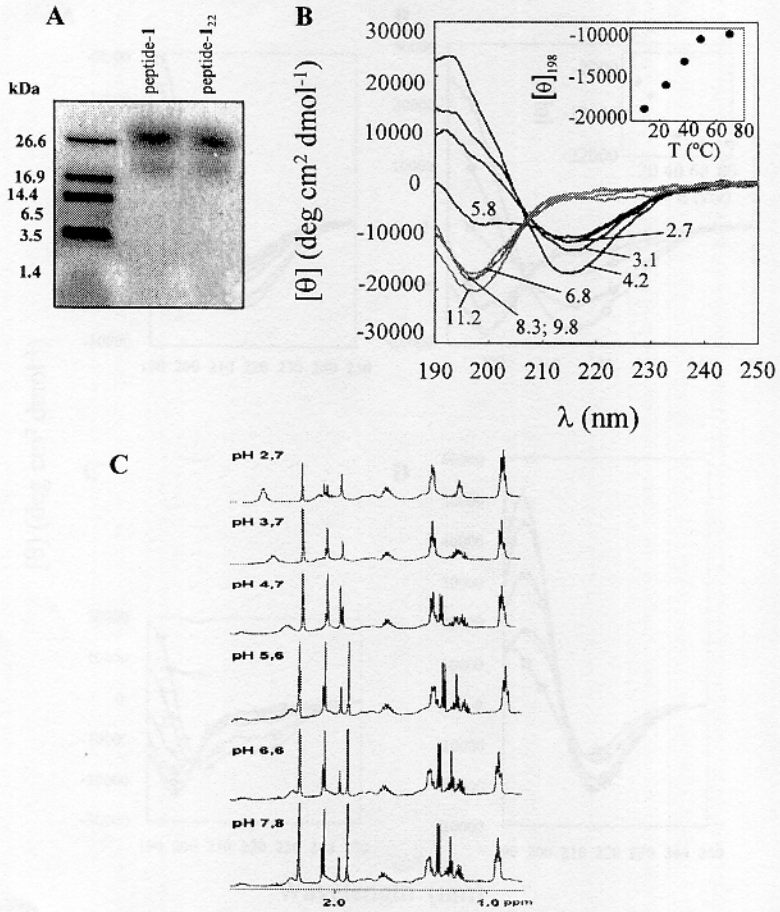

Figure 4

Conformational characterisation of peptide-1. (A). Tris-Tricine electrophoretic mobility of peptide-**1** and peptide-**1**$_{22}$. (see Table 1 for theoretical molecular weights). Standard molecular weight markers are shown on the left. **(B).** far-UV CD spectra as a function of pH at 10°C. The concentration of peptide-**1** was 50 μM. pH values are indicated in the spectra. The insert shows the dependence with the temperature of the molar ellipticity at 198 nm from spectra acquired at pH 6.8. **(C).** ^{1}H NMR monodimensional spectra of peptide-**1** (50 μM) in water at different pH values.

Table 1: Amino acid sequences of synthetic peptide-1 and analogues

Peptide	Sequence	Mw (Da)	Altered electrophoretic mobility[a]
1	Ac-YKTEAETKTEAKVDAKADVE-NH_2	2267	YES
1$_{22}$	Ac-YKTEAETKTEA**AA**KVDAKADVE-NH_2	2410	YES
1$_{18}$	Ac-YEAETKTEAKVDAKADVE-NH_2	2038	YES
1$_{14}$	Ac-YKTEAKVDAKADVE-NH_2	1608	YES
1$_{10}$	Ac-YKVDAKADVE-NH_2	1178	NON

[a] Analysed by means of Tris-tricine electrophoresis (see Material and Methods section). Altered electrophoretic mobility means that the observed electrophoretic mobility is decreased when compared to the expected from the theoretical molecular weight.

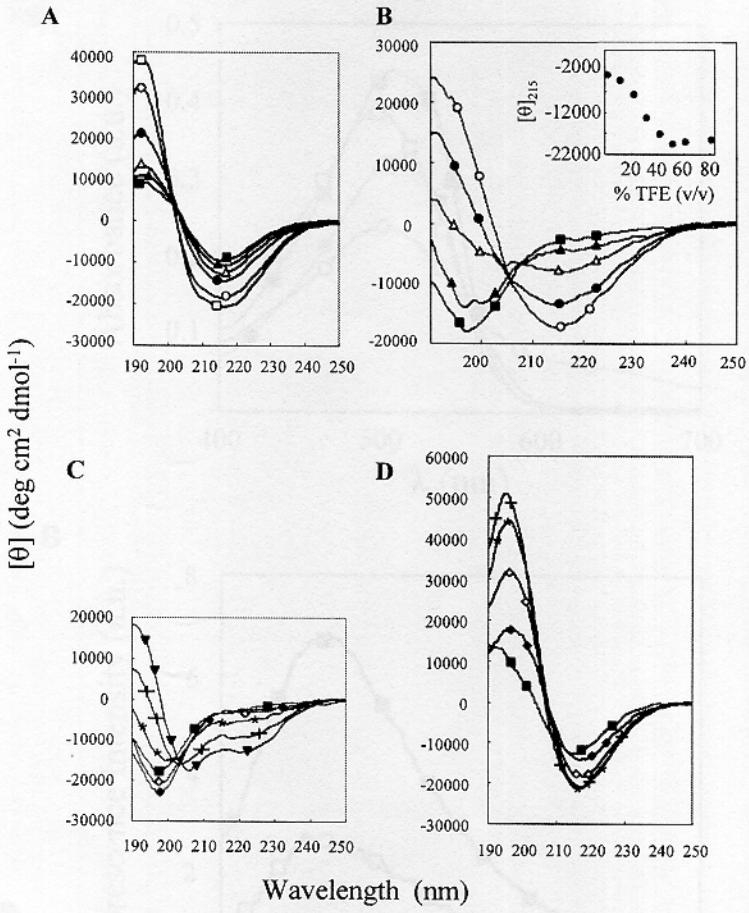

Figure 5

Conformational characterisation of peptide-1 at 10°C in the presence of TFE and SDS (A). Far-UV CD spectra at pH 4.2 as a function of TFE concentration. TFE induces a decrease in the molar ellipticity at 215 nm (CD spectra acquired at ■, 0 %; ▲, 10 %; Δ, 20 %; ●, 30 %; ○, 40 %, and □ 60 %, v/v, TFE concentrations). **(B).** Far-UV CD spectra at pH 6.8 at different TFE concentrations (symbols as in panel A). The insert shows the dependence with TFE concentration (v/v) of the molar ellipticity at 215 nm. **(C).** Far-UV CD spectra at pH 6.8 at different SDS concentrations (■, 0 mM; ◆, 1 mM, ◇, 2 mM; Æ, 3 mM; + 5 mM and ▼, 10 mM). **(D).** Far-UV CD spectra at pH 3.2 at different SDS concentrations (symbols as in part **C**). The concentration of peptide-1 in all the spectra was 50 μM.

istic of β-sheet structure (Fig. 5B and insert). The conformational transition of peptide-1 was also analysed in the presence of SDS, which is considered a template that would stabilize both α-helical and β-sheet conformations depending on the intrinsic propensity of the polypeptide sequence to adopt a preferred secondary structure [31]. At neutral pH concentrations of SDS below 2 mM induced the stabilization of the extended (beta) structure in peptide-1, whereas higher SDS concentrations induced an α-helical conformation (Fig. 5C). At acidic pH values, it has been shown that peptide-1 adopts a β-sheet conformation that renders CD spectra characterized by a minimum at 215 nm (Fig. 4B). When the influence of SDS on the conformational transition of peptide-1 was analyzed at pH 3.2 a further increase in the characteristics that define the canonical CD spectra associated to the β-sheet conformation was obtained. In this sense, both the ellipticity at 215 nm (in absolute value) and at 198 nm increased (Fig. 5D).

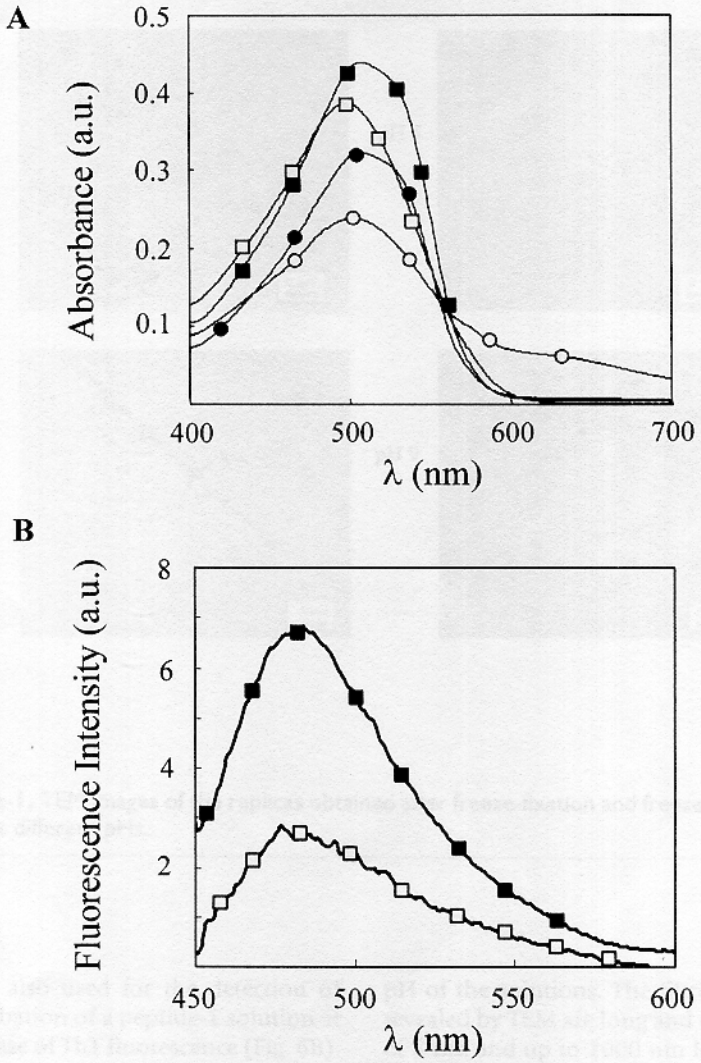

Figure 6

Evidence for amyloid-like fibrils formed by peptide-1. (A). Visible spectra of the Congo red dye at two different pH values (circles pH 4.2 and squares pH 7.2) in the absence (empty symbols) and in the presence (filled symbols) of 50 μM of peptide-**1**. **(B).** Thioflavin T (10 μM) emission fluorescence spectra in Tris-HCl 20 mM pH 7.2 buffer in the absence (empty squares) and in the presence of peptide-**1** at 200 μM (filled squares).

Amyloid-like fibril formation of peptide-1

The NMR and CD data suggest that peptide-**1** can exist in solution as a complex mixture of conformations that could extend from low molecular weight and unstructured species to large oligomers with a predominant secondary structure in β-sheet. This prompted us to expand our studies by using tools able to diagnose fibril formation.

Spectroscopic binding assays of peptide-**1** at 50 μM to the diazo dye Congo red at two different pH values (Fig. 6A) show the typical red shift in wavelength and increase in intensity characteristic of amyloid-like fibrils [32]. The

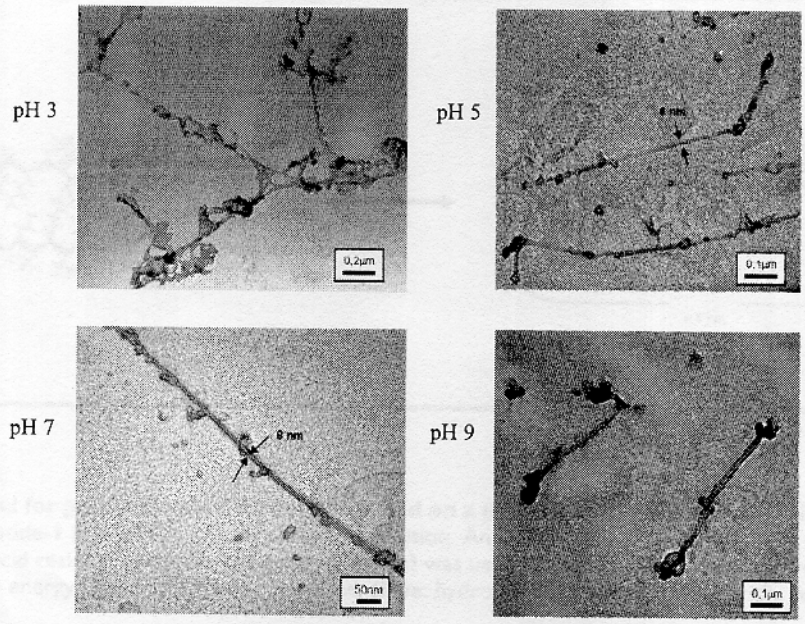

Figure 7
TEM images for peptide-1. TEM images of the replicas obtained after freeze-fixation and freeze-drying of a 100 µM aqueous solution of the peptide-**1** at different pHs.

dye tioflavin T (ThT) is also used for the detection of amyloid fibrils [33]. Incubation of a peptide-**1** solution at pH 7.5 produces an increase of ThT fluorescence (Fig. 6B). The oligomeric state of peptide-1 in solution was determined by analytical ultracentrifugation. At 10°C the sedimentation analysis (not shown) allowed the determinations of the Svedverg coefficients for peptide-**1** (50 µM) at pH 4.1 and pH 8, which are compatible with molecular weights between 300 and 1000 kDa. These results suggest that peptide-**1**, at neutral and acidic pH values, has a high tendency to form high molecular weight aggregates that have amyloid-like fibril characteristics.

In order to further characterise the aggregation process of peptide-1 in solution, eight different preparations of peptide solutions were freeze-fixed and freeze-dried to preserve the aggregate structures in solution for subsequent transmission electron microscopy (TEM) imaging. Two solutions at 10 and 100 µM of peptide-**1** were prepared and divided in four fractions, being each fraction adjusted to different pH values (3, 5, 7 and 9) with HCl or NaOH. Different kinds of aggregates were observed depending on pH of the solutions. The fibrils obtained at pH 5 and 7 revealed by TEM are long and unbranched with diameters of 8 nm and up to 1000 nm length (Fig. 7). This fibrillar material appears similar to the protofilaments observed in other amyloidogenic systems [34,35]. In contrast at pH 3 and 9 peptide-**1** aggregates giving irregular structures (Fig. 7).

Discussion

In previous work, we have shown that the *Arabidopsis thaliana* copper metallochaperone CCH, the functional homologue of yeast Atx1, contains an extra C-terminal domain with unusual structural properties. This domain has a folding pathway independent from the N-terminal domain and it confers to the whole CCH protein an altered electrophoretic mobility in SDS-PAGE [13]. In the present study, we have further characterized the CCH C-domain and delimited a peptide that accounts for most of its structural properties such as its high tendency to form oligomers. We also show that such peptide oligomerizes to form amyloid-like fibrils and that β-strand structure in

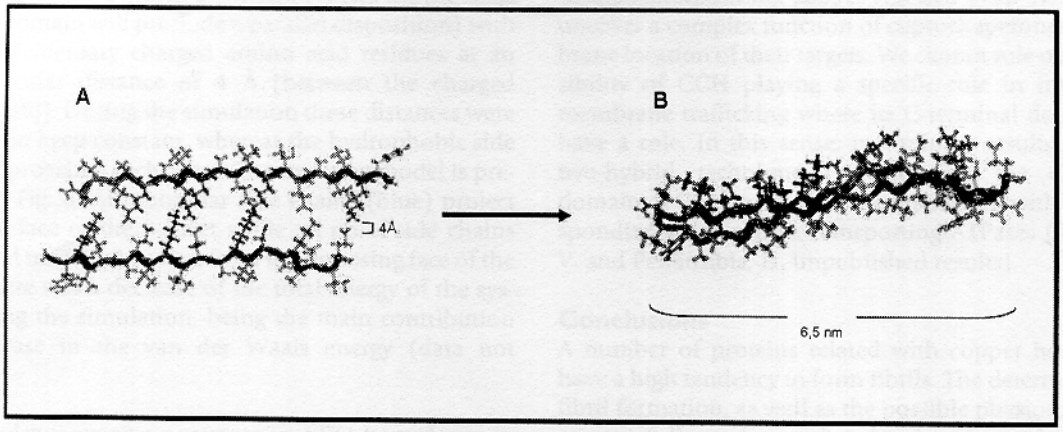

Figure 8
Hypothetical model for peptide-1 fibril formation based on a molecular dynamics simulation. (A) Initial structure with two units of peptide-**1** arranged in a β-antiparallel disposition. An intermolecular distance of 4 Å within the complementary charged amino acid residues (between the charged atoms) was used. **(B).** Snapshot representative of the final part of the simulation where the energy of the system was stabilized. (Blue: hydrophobic residues, green: acidic residues; magenta: basic residues).

solution and self-complementary attractive electrostatic interactions could be a requirement for fibrillogenesis.

The recombinant C-domain adopts an extended (beta) structure in solution at acidic, neutral and basic pH that induces the formation of fibril structures as determined by TEM. Furthermore, as demonstrated by altered electrophoretic mobility [14] and analytical ultracentrifugation (Fig. 3) the C-domain shows tendency to participate in SDS-induced oligomerization events.

A synthetic peptide (peptide-**1** – Fig. 1) derived from the C-domain was selected in order to facilitate the conformational study. Peptide-**1** has most of the general sequence properties of the C-domain. It is characterised by a pattern of alternating hydrophobic and hydrophilic residues and by a striking overall charge distribution containing a 30% and 20% of negative and positively charged residues, respectively, with a pI value of 4.8 (the C-domain has 27% and 15%, respectively, with a pI value of 4.5). Furthermore, peptide-**1** showed an altered electrophoretic mobility (Fig. 4A). The minimal length of the peptide that confers this property is 14 amino acids, as determined by a series of deletion peptides (Table 1). It is well known that pH changes have drastic effects on protein and peptide structures and in particular in peptides that form supramolecular structures. The β-amyloid peptide undergoes conformational change as function of pH. At pH 1.3 and 8.3, adopts a helical conformation, whereas at pH 5.4 it has a β-sheet structure [36]. In the same manner, the ionic self-complementary peptides developed by Zhang and Rich [21,22,37,38] undergo similar structural changes. Peptide-**1**, when protonated below pH 4, has a CD spectrum characteristic of a canonical β-sheet, similar to that reported for the ionic self-complementary peptide EAK12-d (pI 4.5 – [22]). The structural transition of peptide-1 towards an extended (beta) structure takes place at about pH 5, near its pI value, with an intermediate spectrum (Fig. 4A). Analytical ultracentrifugation demonstrated that in the two pH-dependent conformations peptide-**1** forms large oligomers that showed to have amyloid-like properties as is the ability to bind to Congo red and thioflavin T (Fig. 6) and to form fibrils (Fig. 7). The analysis by TEM of the fibrils obtained from freeze-fixed and freeze-dried of peptide-**1** solutions at neutral pH showed a regular shape and are long, up to 1000 nm length, and unbranched. However, when the aggregates are prepared from peptide-1 solutions at acidic pH they showed to be more irregular in shape. If the fibrils are composed of the peptide-1 in antiparallel β-sheet conformation, their width should be 6.5 nm in close agreement with the observed average diameter of 8 nm (Fig. 7). Although the detailed structure of fibrils is not available at the moment, a likely model structure of the β-sheet disposition of two peptide-**1** molecules was obtained by molecular dynamics. Initially, two peptide-1 molecules in a β-sheet conformation (see Materials and Methods section) were arbitrarily arranged in an antiparallel disposition

(here we speculated that in the whole protein the presence of the N-domain will preclude a parallel disposition) with the complementary charged amino acid residues at an intermolecular distance of 4 Å (between the charged atoms – [39]). During the simulation these distances were observed to keep constant, whereas the hydrophobic side chains approached each other. The resulting model is presented in Fig. 8. All nonpolar side chains (blue) project from one face of the β-sheet while all polar side chains (green and magenta) project from the opposing face of the sheet. There was a decrease of the total energy of the system during the simulation, being the main contribution the decrease in the van der Waals energy (data not shown).

The *Arabidopsis* genome possesses an ATX1 homologue in addition to the plant exclusive CCH protein. It is reasonable to assume that the ATX1 homologue would perform the function of copper delivery to the secretory pathway transporter described in yeast [11]. Since CCH has an exclusive C-domain, absent in the non-plant homologues and it probably reaches its location at the phloem sieve elements through plasmodesmata (the plant intercellular symplastic connections), we have postulated that the C-domain could accomplish this exclusive plant function [13]. Extra C-domains have been also found in other plant cuprochaperones (Mira et al., unpublished results). In order to transport copper through plasmodesmata, higher plant copper metallochaperones could have been evolved the addition of new protein domains that could facilitate the cell-to-cell export mechanism. Although the mechanistic aspects of the process are not yet solved and no consensus sequences are present in the proteins demonstrated to cross plasmodesmata, several characteristics of the CCH C-domain points to a role in that process. The C-domain and peptide-**1**, have conformational flexibility and can be induced to populate different conformations in different membrane-mimetic media like SDS and TFE (Fig. 5) and at different pH values (Figs. 4B and 5B). Such a conformational flexibility could be relevant to allow a protein transport through plasmodesmata which contain membranous extension of the endoplasmic reticulum [40]. The pH change at the phloem [41] could also serve to modulate the conformational steps required in the transport process. Moreover, it has been postulated that microtubules could also play a role in targeting proteins to plasmodesmata [42] and recently, the microtubules have been related to fibrillation processes. In fact, the formation of the neurodegenerative deposits by the fibrillar β-amyloid peptide is affected by the presence of stable microtubules [43] and α-synuclein, subjected to fibrillar aggregation, exploits its interaction with microtubules to address to a specific cellular location [44]. Recently ATX1 mammalian homologues have been shown to play a role not only in copper delivery but in intracellular trafficking of the corresponding copper ATPases [45]. These results uncover a complex function of cuprochaperones in membrane location of their targets. We cannot rule out the possibility of CCH playing a specific role in intracellular membrane trafficking where its C-terminal domain may have a role. In this sense, preliminary results using the two-hybrid technique indicate that the C-terminal domain of CCH modulates the interaction with the corresponding plant copper-transporting ATPases (Sancenón, V. and Peñarrubia, L., unpublished results).

Conclusions

A number of proteins related with copper homeostasis have a high tendency to form fibrils. The determinants for fibril formation, as well as the possible physiological role are not fully understood. It has been postulated that a problem associated to the interaction between copper binding proteins and biological membranes is the dangerous generation of H2O2 through Cu2+ reduction, which make cells more responsive to oxidative stress [46]. Atx-like metallochaperones have a copper-binding motif and antioxidant properties [47,48] related to the CCH N-domain [10], while the domain implicated in the fibrillation process is the C-domain. The putative reciprocal influence between these properties should be addressed in the whole protein.

Methods

Expression and purification of the C-domain of CCH

The recombinant C-domain of CCH was expressed and purified from *Escherichia coli* DH5α cells as previously reported [14].

Sequence analysis

Secondary structure predictions were determined using the PHD software (EMBL, Heidelberg, Germany) and the program AGADIR [29].

Peptide synthesis

Peptides were synthesized by solid-phase multiple peptide synthesis [49] using Fmoc chemistry [50] and purified by reversed-phase high performance liquid chromatography (RP-HPLC) using a C_{18} column. Analytical RP-HPLC and laser desorption time-of-flight mass spectrometry were used to determined the purity and identity of the peptides.

Circular dichroism spectroscopy

All measurements were carried out on a Jasco J-810 CD spectropolarimeter, in conjunction with a Neslab RTE 110 waterbath and temperature controller. CD spectra were the average of a series of ten scans made at 0.2 nm intervals. CD spectra of the same buffer (or in the presence of trifluorethanol (TFE) or sodium dodecyl sulfate (SDS) as described in the Figure Legends) without peptide were

used as baseline in all the experiments. For peptide-1 and analogues the concentration was determined by UV spectrophotometry using $\varepsilon_{276,Tyr}$ = 1450 $M^{-1}cm^{-1}$. The concentration of the C-domain was obtained by quantitative amino acid analysis.

Analytical ultracentrifugation

Sedimentation equilibrium analysis of the CCH C-domain was performed using a Beckman XL-I analytical ultracentrifuge. Three solutions of the C-domain at concentrations of 0.9, 0.45 and 0.23 mg/mL were prepared in 50 mM Tris-HCl pH 8.0, containing 0.2 M NaCl and centrifugated at 50000 rpm. An additional solution of the C-domain at 0.5 mg/mL was also prepared in the presence of 1 mM SDS, and centrifuged at 45000 rpm, at 25 °C. The equilibrium was determined when successive radial absorbance scans at the same speed were indistinguishable. Partial specific volumes and molecular weights were estimated for the C-domain using the software Sedinterp [51]. The amino acid partial specific volumes were updated using the values reported by Kharakoz [52]. For the C-domain the calculated values were 0.7404 mL/mg and 4936.6 Da. Solution density was estimated to be 1.00781 g/mL also using "Sedinterp". Data obtained by UV absorbance were analyzed by non-linear least squares curve fitting of radial concentration profiles using the Marquardt-Levenberg algorithm implemented in Igor Pro (Wavemetrics, Oswego, OR) with a user-defined function, as previously described [53]. Sedimentation equilibrium analysis of peptide-1 was performed at the Analytical Ultracentrifugacion Facility, Centro de Investigaciones Biológicas, CSIC, Madrid.

NMR spectroscopy

NMR spectra were recorded using a Bruker AMX-500 (500 MHz ^1H) NMR spectrometer. ^1H NMR spectra were acquired using H_20 10% D_2O as solvent at 298 K. The pH of the solutions was adjusted with solutions of 10 mM HCl or 10 mM NaOH.

Congo red and thioflavine T binding analysis

For the Congo red (Merck) binding assay of fibril formation, absorption spectra of 10 μM solution of the dye at different pH values before and after addition of the peptide-1 solution (final concentration 50 μM) were recorded in a Cintra 10 e spectrometer (GBC Sci. Equip., Australia). For the thioflavine T (Aldrich) binding assay, fluorescence emission spectra of 10 μM solution (in Tris-HCl 25 mM pH 7.2 buffer) of the dye were measured before and after addition of the peptide-1 solution (final concentration 200 μM) on a Perkin-Elmer (Beaconsfield, UK.) LS-5B spectrofluorimeter at excitation wavelength of 440 nm. The bandwidths of excitation and emission were 5 nm.

Freeze fixation, freeze drying electron microscopy

Drops of recombinant C-domain or peptide-**1** solutions (see text) were deposited over uncoated coverslips. Coverslips were cryofixed by projection against a copper block cooled by liquid nitrogen (-196 °C) using a cryoblock (Reicher-Jung, Leica). The frozen samples were stored at -196 °C in liquid nitrogen until subsequent use. Samples were freeze-dried at -90 °C and coated with platinum and carbon using a freeze-etching unit (model BAF-060, BALTEC, Liechtenstein). A rotatory shadowing of the exposed surface was made by evaporating 1 nm platinum-carbon at an angle of six degrees above the horizontal, followed by 10 nm of carbon evaporated at an angle of ninety degrees. The replica was separated from the coverslip by immersion in concentrated hydrofluoric acid, washed twice in distilled water and digested with 5 % sodium hydrochloride for 5 – 10 minutes. Finally, the replicas were washed several times in distilled water, broken into small pieces and collected on Formvar-coated copper grids for electron microscopy. All electron micrographs were obtained using an electron microscope Hitachi 800 MT operating at 75 KV. Up to ten different samples were prepared by this procedure and the results were reproducible among all the samples assayed.

Molecular dynamics

The molecular dynamics simulation was carried out at 300 K during 1000 ps at pH 7 and ε = 4r using CVFF (implemented in DISCOVER_3) as force field. The torsion angles of one unit of peptide-1 backbone were restrained to values between -180° and -60° for the ϕ angle and between 180° and 80° for the ϕ angle (typical β-sheet range in a Ramachandran plot). Two peptide-**1** molecules in an antiparallel arrangement were selected to run the molecular dynamics simulation. This arrangement of the peptide molecules allows the putative formation of a maximised number of both salt bridges and hydrogen bonds.

Authors' contributions

HM initiated this project as part of her PhD and analyzed the cell biology aspects. MV was in charge of the synthetic and electrophoretical aspects of the peptides and fluorescence and CD spectroscopies. VE and MM contributed to the NMR. MJK was in charge of the electronic microscope experiments and with MM contributed to generate the C-domain model. EG coordinates the NMR and modelling studies and participates in the redaction and discussion of the manuscript with IM and LP. The whole work was coordinated by EPP.

Acknowledgements

This work was supported by grants BIO4-CT97-2086 (EU Biotechnology), SAF01-2811, BIO2002-1125 and BIO2002-2301 (MCyT and FEDER), and Generalitat de Catalunya (Grups Consolidats de Recerca and Centre de Referència en Biotecnologia). We are grateful to Dr. William DeGrado (Univ. Pennsylvania) for the use of the Beckman XL-I analytical ultracentri-

fuge. We thank Alicia García and Ana Giménez for excellent technical work.

References

1. Broome BM, Hecht MH: **Nature disfavors sequences of alternating polar and non-polar amino acids: implications for amyloidogenesis.** *J Mol Biol* 2000, **296:**961-968.
2. Kelly JW: **The alternative conformations of amyloidogenic proteins and their multi-step assembly pathways.** *Curr Opin Struct Biol* 1998, **8:**101-106.
3. Konno T, Murata K, Nagayama K: **Amyloid-like aggregates of a plant protein: a case of a sweet-tasting protein, monellin.** *FEBS Lett* 1999, **454:**122-126.
4. Konno T: **Multistep nucleus formation and a separate subunit contribution of the amyloidgenesis of heat-denatured monellin.** *Protein Sci* 2001, **10:**2093-2101.
5. Opazo C, Huang X, Cherny RA, Moir RD, Roher AE, White AR, Cappai R, Masters CL, Tanzi RE, Inestrosa NC, Bush AI: **Metalloenzyme-like activity of Alzheimer's disease beta-Amyloid. Cu-dependent catalytic conversion of dopamine, cholesterol, and biological reducing agents to neurotoxic H2O2.** *J Biol Chem* 2002, **277:**40302-40308.
6. Johnston JA, Dalton MJ, Gurney ME, Kopito RR: **Formation of high molecular weight complexes of mutant Cu, Zn-superoxide dismutase in a mouse model for familial amyotrophic lateral sclerosis.** *Proc Natl Acad Sci U S A* 2000, **97:**12571-12576.
7. Pauly PC, Harris DA: **Copper stimulates endocytosis of the prion protein.** *J Biol Chem* 1998, **273:**33107-33110.
8. Wong BS, Venien-Bryan C, Williamson RA, Burton DR, Gambetti P, Sy MS, Brown DR, Jones IM: **Copper refolding of prion protein.** *Biochem Biophys Res Commun* 2000, **276:**1217-1224.
9. Brown DR, Wong BS, Hafiz F, Clive C, Haswell SJ, Jones IM: **Normal prion protein has an activity like that of superoxide dismutase.** *Biochem J* 1999, **344:**1-5.
10. Himelblau E, Mira H, Lin SJ, Culotta VC, Peñarrubia L, Amasino RM: **Identification of a functional homolog of the yeast copper homeostasis gene ATX1 from Arabidopsis.** *Plant Physiol* 1998, **117:**1227-1234.
11. Lin SJ, Culotta VC: **The ATX1 gene of Saccharomyces cerevisiae encodes a small metal homeostasis factor that protects cells against reactive oxygen toxicity.** *Proc Natl Acad Sci U S A* 1995, **92:**3784-3788.
12. Yuan DS, Dancis A, Klausner RD: **Restriction of copper export in *Saccharomyces cerevisiae* to a late Golgi or post-Golgi compartment in the secretory pathway.** *J Biol Chem* 1997, **272:**25787-25793.
13. Mira H, Martinez-Garcia F, Peñarrubia L: **Evidence for the plant-specific intercellular transport of the Arabidopsis copper chaperone CCH.** *Plant J* 2001, **25:**521-528.
14. Mira H, Vilar M, Pérez-Payá E, Peñarrubia L: **Functional and conformational properties of the exclusive C-domain from the Arabidopsis copper chaperone (CCH).** *Biochem J* 2001, **357:**545-549.
15. West MW, Wang W, Patterson J, Mancias JD, Beasley JR, Hecht MH: **De novo amyloid proteins from designed combinatorial libraries.** *Proc Natl Acad Sci U S A* 1999, **96:**11211-11216.
16. Wang W, Hecht MH: **Rationally designed mutations convert de novo amyloid-like fibrils into monomeric beta-sheet proteins.** *Proc Natl Acad Sci U S A* 2002, **99:**2760-2765.
17. Macias MJ, Gervais V, Civera C, Oschkinat H: **Structural analysis of WW domains and design of a WW prototype.** *Nat Struct Biol* 2000, **7:**375-379.
18. Landrieu I, Wieruszeski JM, Wintjens R, Inze D, Lippens G: **Solution structure of the single-domain prolyl cis/trans isomerase PIN1At from *Arabidopsis thaliana*.** *J Mol Biol* 2002, **320:**321-332.
19. Kanelis V, Rotin D, Forman-Kay JD: **Solution structure of a Nedd4 WW domain-ENaC peptide complex.** *Nat Struct Biol* 2001, **8:**407-412.
20. Pastor MT, Lopez de la Paz M, Lacroix E, Serrano L, Pérez-Payá E: **Combinatorial approaches: a new tool to search for highly structured beta-hairpin peptides.** *Proc Natl Acad Sci U S A* 2002, **99:**614-619.
21. Zhang S, Rich A: **Direct conversion of an oligopeptide from a beta-sheet to an alpha-helix: a model for amyloid formation.** *Proc Natl Acad Sci U S A* 1997, **94:**23-28.
22. Altman M, Lee P, Rich A, Zhang S: **Conformational behavior of ionic self-complementary peptides.** *Protein Sci* 2000, **9:**1095-1105.
23. Hames BD: **An introduction to polyacrylamide gel electrophoresis.** In *gel electrophoresis: a practical approach* Edited by: Hames BD, Rickwood D. Washington DC: Oxford IRL Press; 1981:1-86.
24. Jones DH, Ball EH, Sharpe S, Barber KR, Grant CW: **Expression and membrane assembly of a transmembrane region from Neu.** *Biochemistry* 2000, **39:**1870-1878.
25. Kaufmann E, Geisler N, Weber K: **SDS-PAGE strongly overestimates the molecular masses of the neurofilament proteins.** *FEBS Lett* 1984, **170:**81-84.
26. Orzáez M, Pérez-Payá E, Mingarro I: **Influence of the C-terminus of the glycophorin A transmembrane fragment on the dimerization process.** *Protein Sci* 2000, **9:**1246-1253.
27. Zhong L, Johnson WC Jr: **Environment affects amino acid preference for secondary structure.** *Proc Natl Acad Sci U S A* 1992, **89:**4462-4465.
28. Steele JC Jr, Tanford C, Reynolds JA: **Determination of partial specific volumes for lipid-associated proteins.** *Methods Enzymol* 1978, **48:**11-23.
29. Muñoz V, Serrano L: **Development of the multiple sequence approximation within the AGADIR model of alpha-helix formation: comparison with Zimm-Bragg and Lifson-Roig formalisms.** *Biopolymers* 1997, **41:**495-509.
30. Gross M, Wilkins DK, Pitkeathly MC, Chung EW, Higham C, Clark A, Dobson CM: **Formation of amyloid fibrils by peptides derived from the bacterial cold shock protein CspB.** *Protein Sci* 1999, **8:**1350-1357.
31. Blondelle SE, Ostresh JM, Houghten RA, Pérez-Payá E: **Induced conformational states of amphipathic peptides in aqueous/lipid environments.** *Biophys J* 1995, **68:**351-359.
32. Klunk WE, Pettegrew JW, Abraham DJ: **Quantitative evaluation of congo red binding to amyloid-like proteins with a beta-pleated sheet conformation.** *J Histochem Cytochem* 1989, **37:**1273-1281.
33. LeVine H 3rd: **Quantification of beta-sheet amyloid fibril structures with thioflavin T.** *Methods Enzymol* 1999, **309:**274-284.
34. Chiti F, Webster P, Taddei N, Clark A, Stefani M, Ramponi G, Dobson CM: **Designing conditions for in vitro formation of amyloid protofilaments and fibrils.** *Proc Natl Acad Sci U S A* 1999, **96:**3590-3594.
35. Tjernberg LO, Tjernberg A, Bark N, Shi Y, Ruzsicska BB, Bu Z, Thyberg J, Callaway DJ: **Assembling amyloid fibrils from designed structures containing a significant amyloid beta-peptide fragment.** *Biochem J* 2002, **366:**343-351.
36. Barrow CJ, Zagorski MG: **Solution structures of beta peptide and its constituent fragments: relation to amyloid deposition.** *Science* 1991, **253:**179-182.
37. Zhang S, Lockshin C, Cook R, Rich A: **Unusually stable beta-sheet formation in an ionic self-complementary oligopeptide.** *Biopolymers* 1994, **34:**663-672.
38. Zhang S, Holmes T, Lockshin C, Rich A: **Spontaneous assembly of a self-complementary oligopeptide to form a stable macroscopic membrane.** *Proc Natl Acad Sci U S A* 1993, **90:**3334-3338.
39. Ciani B, Jourdan M, Searle M: **Stabilization of beta-hairpin peptides by salt bridges: role of preorganization in the energetic contribution of weak interactions.** *J Am Chem Soc* 2003, **125:**9038.
40. Kragler F, Monzer J, Shash K, Xoconostle-Cazares B, Lucas WJ: **Cell-to-cell transport of proteins:requirement for unfolding and characterization of binding to a putative plasmodesmal receptor.** *Plant J* 1998, **15:**367-381.
41. Patrick JW: **Phloem unloading:sieve element unloading and post-sieve element transport.** *Annu Rev Plant Physiol Plant Mol Biol* 1997, **48:**191-222.
42. Boyko V, Ferralli J, Heinlein M: **Cell-to-cell movement of TMV RNA is temperature-dependent and corresponds to the association of movement protein with microtubules.** *Plant J* 2000, **22:**315-325.
43. Rapoport M, Dawson HN, Binder LI, Vitek MP, Ferreira A: **Tau is essential to beta-amyloid-induced neurotoxicity.** *Proc Natl Acad Sci U S A* 2002, **99:**6364-6369.
44. Lee HJ, Lee SJ: **Characterization of Cytoplasmic alpha-Synuclein Aggregates. Fibril formation is tightly linked to the**

inclusion-forming process in cells. *J Biol Chem* 2002, **277:**48976-48983.

45. Hamza I, Prohaska J, Gitlin JD: **Essential role for Atox1 in the copper-mediated intracellular trafficking of the Menkes ATPase.** *Proc Natl Acad Sci U S A* 2003, **100:**1215-1220.
46. Curtain CC, Ali F, Volitakis I, Cherry RA, Norton RS, Beyrenther K, Barrow CJ, Masters CL, Bush AI, Barnham K: **Alzheimer's disease amyloid-beta binds copper and zinc to generate an allosterically ordered membrane-penetrating structure containing superoxide dismutase-like subunits.** *J Biol Chem* 2001, **276:**20466-20473.
47. Portnoy ME, Rosenzweig AC, Rae T, Huffman DL, O'Halloran TV, Culotta VC: **Structure-function analyses of the ATX1 metallochaperone.** *J Biol Chem* 1999, **274:**15041-15045.
48. Hung IH, Casareno RL, Labesse G, Mathews FS, Gitlin JD: **HAH1 is a copper-binding protein with distinct amino acid residues mediating copper homeostasis and antioxidant defense.** *J Biol Chem* 1998, **273:**1749-1754.
49. Houghten RA: **General method for the rapid solid-phase synthesis of large numbers of peptides: specificity of antigen-antibody interaction at the level of individual amino acids.** *Proc Natl Acad Sci U S A* 1985, **82:**5131-5135.
50. Fields GB, Noble RL: **Solid phase peptide synthesis utilizing 9-fluorenylmethoxycarbonyl amino acids.** *Int J Pept Protein Res* 1990, **35:**161-214.
51. Laue T, Shaw BD, Ridgeway TM, Pelletier SL: In: *Analytical Ultracentrifugation in Biochemistry and Polymer Science* Edited by: Harding SE, Rowe AJ, Horton JC. Cambridge, U.K.: The Royal Society of Chemistry; 1992:90-125.
52. Kharakoz DP: **Partial volumes and compressibilities of extended polypeptide chains in aqueous solution: additivity scheme and implication of protein unfolding at normal and high pressure.** *Biochemistry* 1997, **36:**10276-10285.
53. Kochendoerfer GG, Salom D, Lear JD, Wilk-Orescan R, Kent SB, DeGrado WF: **Total chemical synthesis of the integral membrane protein influenza A virus M2: role of its C-terminal domain in tetramer assembly.** *Biochemistry* 1999, **38:**11905-11913.